64

FIGURE 2.11 Measured reduction in apparent power rating (RAPR) of 25 kVA single-phase pole transformer as a function of total harmonic current distortion (THD$_i$) where 3rd and 5th current harmonics are dominant. Calculated values from F_{HL}-factor [12].

The harmonic content of a square wave with magnitude 1.00 pu is known.

a) Develop a Fourier analysis program for any periodic function resulting in the DC offset and the amplitudes of any even and odd harmonics involved.

b) Apply this program to a square wave with magnitude 1.00 pu by taking into account the Nyquist criterion.

c) Plot the original square wave and its Fourier approximation.

d) Compute the K- and F_{HL}-factors by taking various numbers and orders of harmonics into account.

2.3.3.2 Application Example 2.5: K- and F_{HL}-Factors and Their Application to Derating of 25 kVA Single-Phase Pole Transformer Loaded by Variable-Speed Drives

The objective of this example is to apply the computational procedure of Application Example 2.4 to a 25 kVA single-phase pole transformer loaded only by variable-speed drives of central residential air-conditioning systems [16]. Table E2.5.1 lists the mea-

TABLE E2.5.1 Current Spectrum of the Air Handler of a Variable-Speed Drive with (Medium or) 50% of Rated Output Power

I_{DC} (A)	I_1 (A)	I_2 (A)	I_3 (A)	I_4 (A)	I_5 (A)	I_6 (A)
-0.82	10.24	0.66	8.41	1.44	7.27	1.29
I_7 (A)	I_8 (A)	I_9 (A)	I_{10} (A)	I_{11} (A)	I_{12} (A)	I_{13} (A)
4.90	0.97	3.02	0.64	1.28	0.48	0.57
I_{14} (A)	I_{15} (A)	I_{16} (A)	I_{17} (A)	I_{18} (A)	I_{19} (A)	I_{20} (A)
0.53	0.73	0.57	0.62	0.31	0.32	0.14
I_{21} (A)	I_{22} (A)	I_{23} (A)	I_{24} (A)	I_{25} (A)	I_{26} (A)	I_{27} (A)
0.18	0.29	0.23	0.39	0.34	0.39	0.28

sured current spectrum of the air handler of a variable-speed drive with (medium or) 50% of rated output power.

a) Plot the input current wave shape of this variable-speed drive and its Fourier approximation.

b) Compute the K- and F_{HL}-factors and their associated derating of the 25 kVA single-phase pole transformer feeding variable-speed drives of central residential air-conditioning systems. This assumption is a worst-case condition, and it is well-known that pole transformers also serve linear loads such as induction motors of refrigerators and induction motors for compressors of central residential air-conditioning systems.

2.4 NONLINEAR HARMONIC MODELS OF TRANSFORMERS

Appropriate harmonic models of all power system components including transformers are the basis of harmonic analysis and loss calculations. Harmonic models of transformers are devised in two steps: the first is the construction of transformer harmonic model, which is mainly characterized by the analysis of the core nonlinearity (due to saturation, hysteresis, and eddy-current effects), causing nonsinusoidal magnetizing and core-loss currents. The second step involves the relation between model parameters and harmonic frequencies. In the literature, many harmonic models for power transformers have been proposed and implemented. These models are based on one of the following approaches:

- time-domain simulation [17–25],
- frequency-domain simulation [26–29],
- combined frequency- and time-domain simulation [30, 31], and
- numerical (e.g., finite-difference, finite-element) simulation [1, 2, 6, 32–34].

This section starts with the general harmonic model for a power transformer and the simulation techniques for modeling its nonlinear iron core. The remainder of the section briefly introduces the basic concepts and equations involving each of the above-mentioned modeling techniques.

2.4.1 The General Harmonic Model of Transformers

Figure 2.12 presents the physical model of a single-phase transformer. The corresponding electrical and magnetic equations are

$$v_p(t) = R_p i_p(t) + L_p \frac{di_p(t)}{dt} + e_p(t), \qquad (2\text{-}28)$$

$$v_s(t) = R_s i_s(t) + L_s \frac{di_s(t)}{dt} + e_s(t), \qquad (2\text{-}29)$$

$$\Phi_m = BA, \qquad (2\text{-}30)$$

$$B = f_{nonlinear}(H), \qquad (2\text{-}31)$$

$$N_p i_p(t) + N_s i_s(t) = H\ell, \qquad (2\text{-}32)$$

where

- R_p and R_s are the resistances of the primary and the secondary windings, respectively,
- L_p and L_s are the leakage inductances of primary and secondary windings, respectively,
- $e_p(t) = N_p \dfrac{d\Phi_m}{dt}$ and $e_s(t) = N_s \dfrac{d\Phi_m}{dt}$ are the induced voltages of the primary and the secondary windings, respectively,
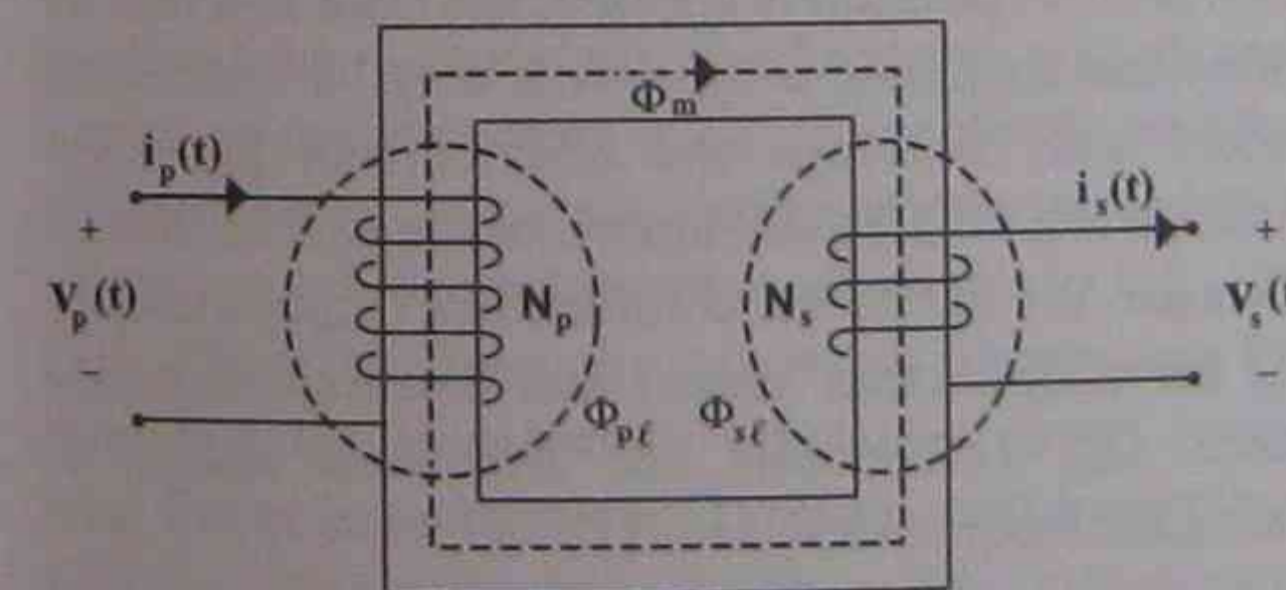- N_p and N_s are the number of turns of the primary and the secondary windings, respectively,
- B, H and Φ_m are the magnetic flux density, the magnetic field intensity, and the magnetic flux in the iron core of the transformer, respectively, and
- A and ℓ are the effective cross section and length of the integration path of transformer core, respectively.

Dividing Eq. 2-32 by N_p yields

$$i_p(t) + \frac{N_s}{N_p} i_s(t) = i_{exc}(t), \qquad (2\text{-}33)$$

where $i_{exc}(t) = H\ell/N_p$ is the transformer excitation (no-load) current, which is the sum of the magnetizing ($i_{mag}(t)$) and core-loss ($i_{core}(t)$) currents. Combining Eqs. 2-30 and 2-31, it is clear that the no-load current is related to the physical parameters, that is, the magnetizing curve (including saturation and hysteresis) and the induced voltage.

Based on Eqs. 2-28, 2-29, and 2-33, the general harmonic model of transformer is obtained as shown in Fig. 2.13. There are four dominant characteristic parameters:

- winding resistance,
- leakage inductance,
- magnetizing current, and
- core-loss current.

Some models assume constant values for the primary and the secondary resistances. However, most references take into account the influence of skin effects and proximity effects in the harmonic model. Since primary ($\Phi_{p\ell}$) and secondary ($\Phi_{s\ell}$) leakage fluxes mainly flow across air, the primary and the secondary leakage inductances can be assumed to be constants. The main difficulty arises in the computation of the magnetizing and core-loss currents, which are the main sources of harmonics in power transformers.
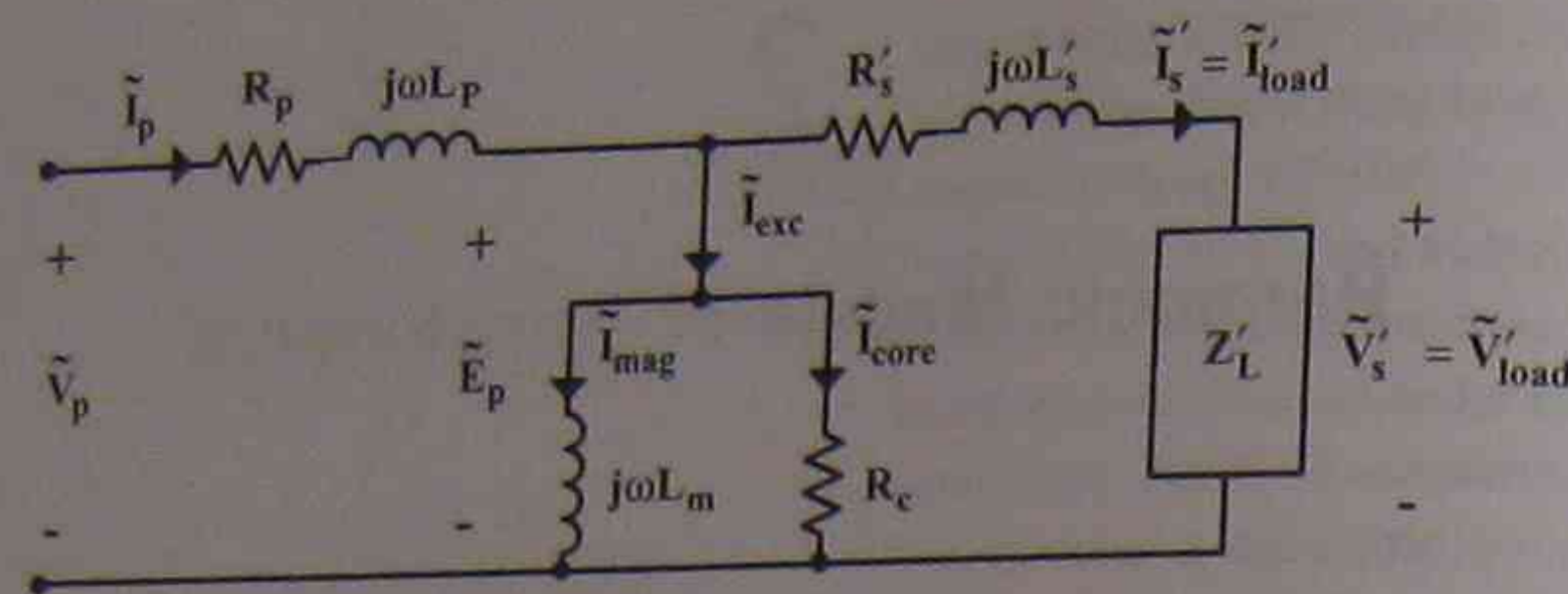

FIGURE 2.12 Physical model of a single-phase transformer.

FIGURE 2.13 General harmonic model of a transformer.

FIGURE 2.1 Linear single-phase, steady-state transformer model for sinusoidal analysis.

Transient models are used for transformer simulation during turning-on (e.g., inrush currents), faults, and other types of disturbances. They are based on a system of time-dependent differential equations usually solved by numerical algorithms. Transient models require a considerable amount of computing time. Steady-state models mostly use phasor analysis in the frequency domain to simulate transformer behavior, and require less computing times than transient models. Transformer modeling for sinusoidal conditions is not the main objective of this chapter. However, Fig. 2.1 illustrates a relatively simple and accurate frequency-based linear model that will be extended to a harmonic model in Section 2.4. In this figure R_c is the core-loss resistance, L_m is the (linear) magnetizing inductance, and R_p, R'_s, L_p, and L'_s are transformer primary and secondary resistances and inductances, respectively. Superscript ' is used for quantities referred from the secondary side to the primary side of the transformer.

The steady-state model of Fig. 2.1 is not suitable for harmonic studies since constant values are assumed for the magnetizing inductance and the core-loss resistance. However, this simple and practical frequency-based model generates acceptable results if a transformer were to operate in the linear region of the $\lambda - i$ characteristic, and the harmonic frequency is taken into account.

2.2 HARMONIC LOSSES IN TRANSFORMERS

Losses due to harmonic currents and voltages occur in windings because of the skin effect and the proximity effect. It is well known that harmonic current $i_h(t)$ and harmonic voltage $v_h(t)$ must be present in order to produce harmonic losses

$$p_h(t) = i_h(t) \cdot v_h(t). \tag{2-2}$$

If either $i_h(t)$ or $v_h(t)$ are zero then $p_h(t)$ will be zero as well. Harmonic losses occur also in iron cores due to hysteresis and eddy-current phenomena. For linear (B–H) characteristics of iron cores, the losses
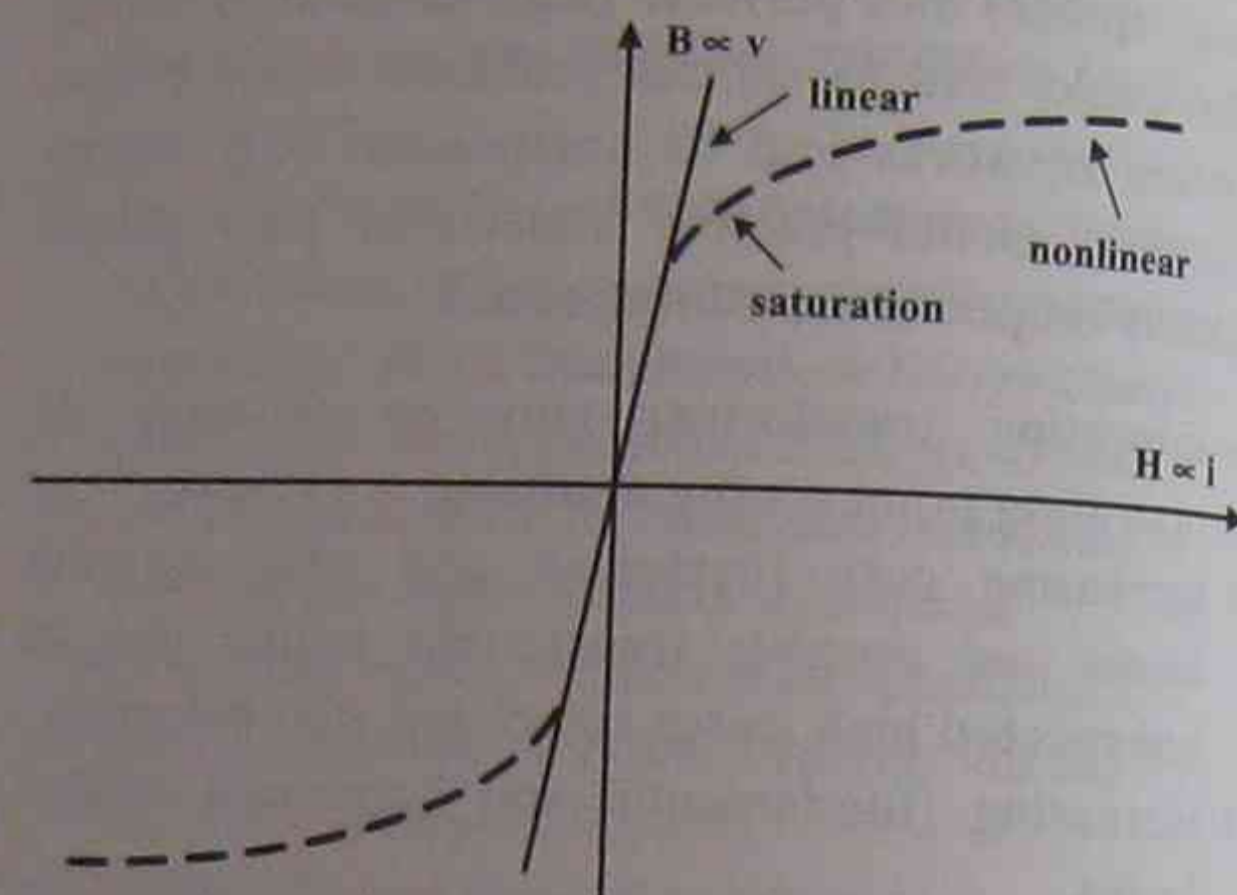

FIGURE 2.2 Linear and nonlinear iron-core characteristics.

are dependent on fundamental and harmonic amplitudes only, whereas for nonlinear iron-core (B–H) characteristics (Fig. 2.2) the phase shift between harmonic voltage and fundamental voltage is important as well. For example, a magnetizing current with maximum peak-to-peak values results in larger maximum flux densities than a magnetizing current with minimum peak-to-peak values. Proximity losses in windings and (solid) conducting parts of a device (e.g., frame) occur due to the relative location between the various windings and conductive parts.

2.2.1 Skin Effect

If a conductor with cross section a_{cond} conducts a DC current I_{DC}, the current density $j_{DC} = I_{DC}/a_{cond}$ is uniform within the conductor and a resistance R_{DC} can be assigned to the conductor representing the ratio between the applied voltage V_{DC} and the resulting current I_{DC}, that is,

$$R_{DC} = \frac{V_{DC}}{I_{DC}}. \tag{2-3}$$

For (periodic) AC currents $i_{ACh}(t)$, the current flows predominantly near the surface of the conductor and the current density j_{ACh} is nonuniform within the conductor (Fig. 2.3). In general,
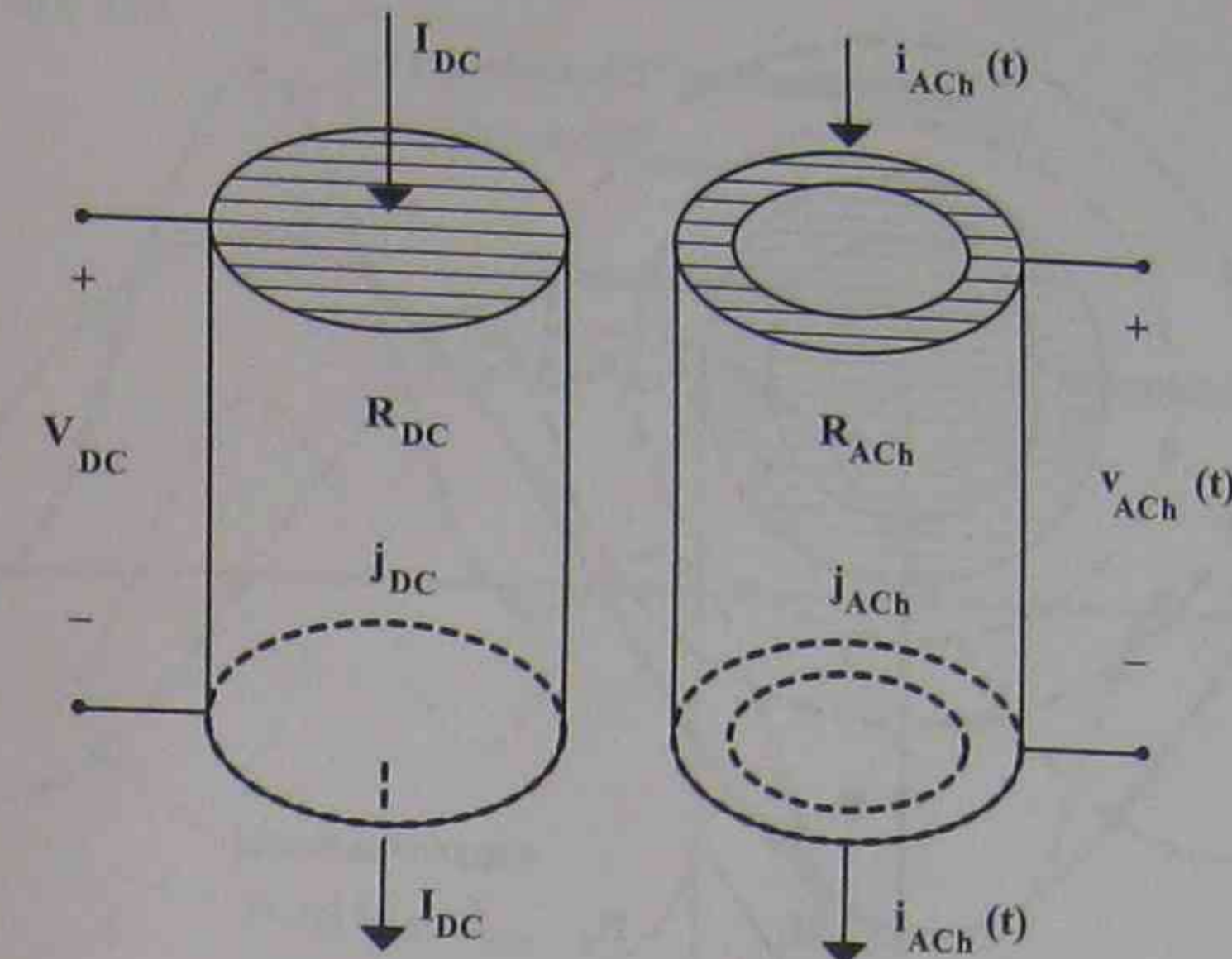
FIGURE 2.3 DC resistance R_{DC} versus AC resistance R_{ACh}.

$$R_{DC} < R_{ACh}.$$

The higher the order h of the harmonic current $i_{ACh}(t)$, the larger is the skin effect.

2.2.2 Proximity Effect

The AC current distribution within a conductor depends on the current distribution of neighboring conductors or conducting parts. The AC field $\vec{H}$ of a single conductor in free space consists of circles symmetric to the axis of the conductor.

$$\text{Ampere's law: } \int \vec{H} \cdot d\vec{l} = \int_S \vec{J} \cdot d\vec{s}. \tag{2-4}$$

If there are two conductors or more, the circular fields will be distorted and the resulting eddy-current losses within the conductor will differ from those of single conductors. In Figs. 2.4 and 2.5, H stands for $|\vec{H}|$.

2.2.3 Magnetic Iron-Core (Hysteresis and Eddy-Current) Losses

All magnetic materials exhibit saturation and hysteresis properties: there are major loops and minor loops (Fig. 2.6) and such characteristics are multivalued for either a single H or a single B value. Therefore, even if there is a sinusoidal input voltage to a magnetic circuit and no minor B–H loops are assumed, a nonsinusoidal current and increased losses are generated. For nonsinusoidal excitation and/or nonlinear loads, excessive magnetic and (fundamental and harmonic) copper losses

may result that could cause transformer failure. In most cases hysteresis losses can be neglected because they are relatively small as compared with copper losses. However, the nonlinear saturation behavior must be taken into account because all transformers and electric machines operate for economic reasons beyond the knee of saturation.

Faraday's law

$$e(t) = \frac{d\lambda(t)}{dt}, \tag{2-5}$$

or

$$\lambda(t) = \int e(t)dt, \tag{2-6}$$

is valid, where $e(t)$ is the induced voltage of a winding residing on an iron core, $\lambda(t) = N\Phi(t)$ are the flux linkages, N is the number of turns of a winding, and $\Phi(t)$ is the flux linked with the winding.

Depending on the phase shift of a harmonic voltage with respect to the fundamental voltage the resulting wave shape of the flux linkages will be different and not proportional to the resulting voltage wave shape due to the integral relationship between flux linkages $\lambda(t)$ and induced voltage $e(t)$ [1–6].

2.2.3.1 Application Example 2.1: Relation between Voltages and Flux Linkages for 0° Phase Shift between Fundamental and Harmonic Voltages

Third harmonic voltage $e_3(t)$ is in phase (0°) with the fundamental voltage $e_1(t)$ resulting in a maximum
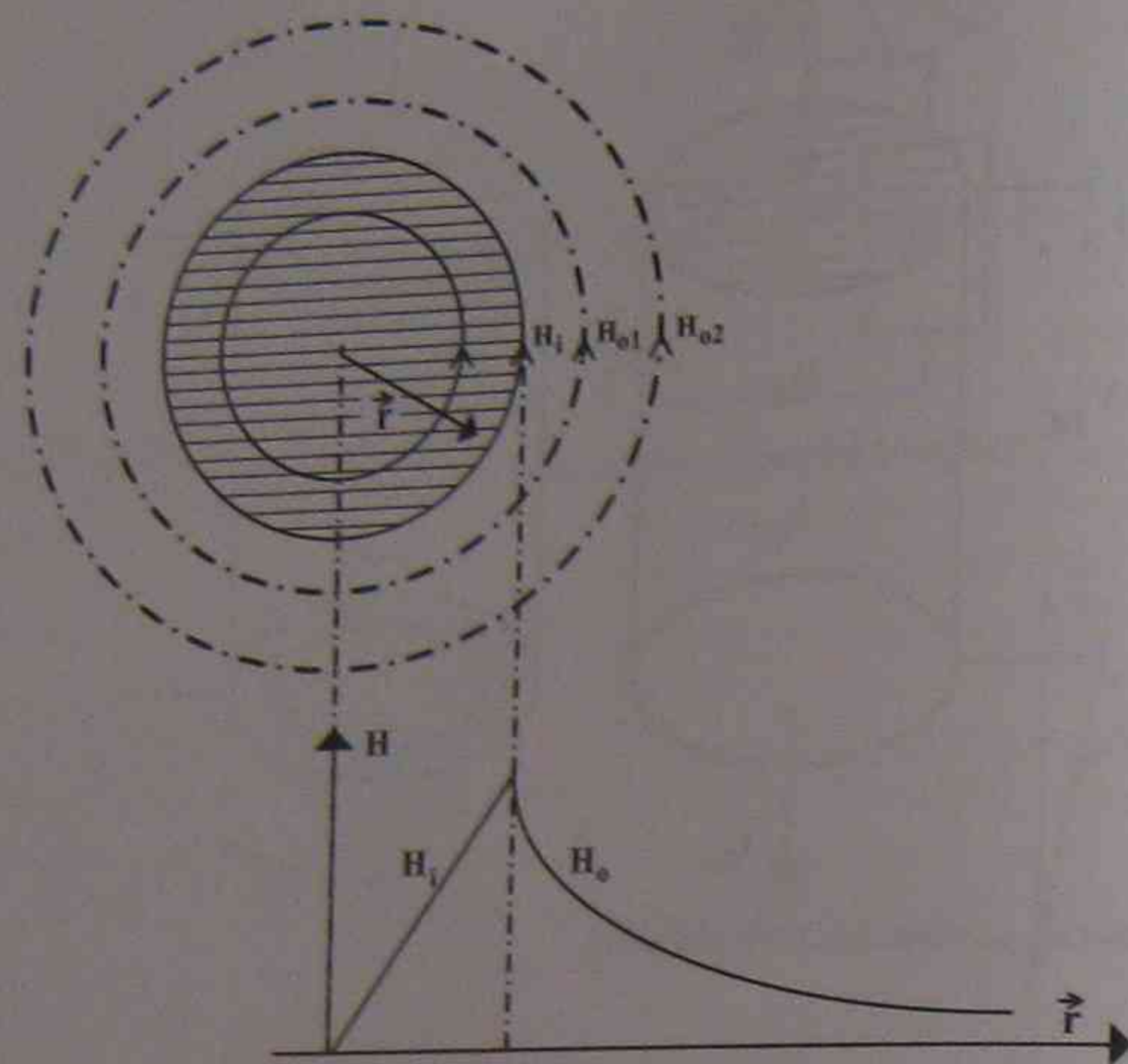
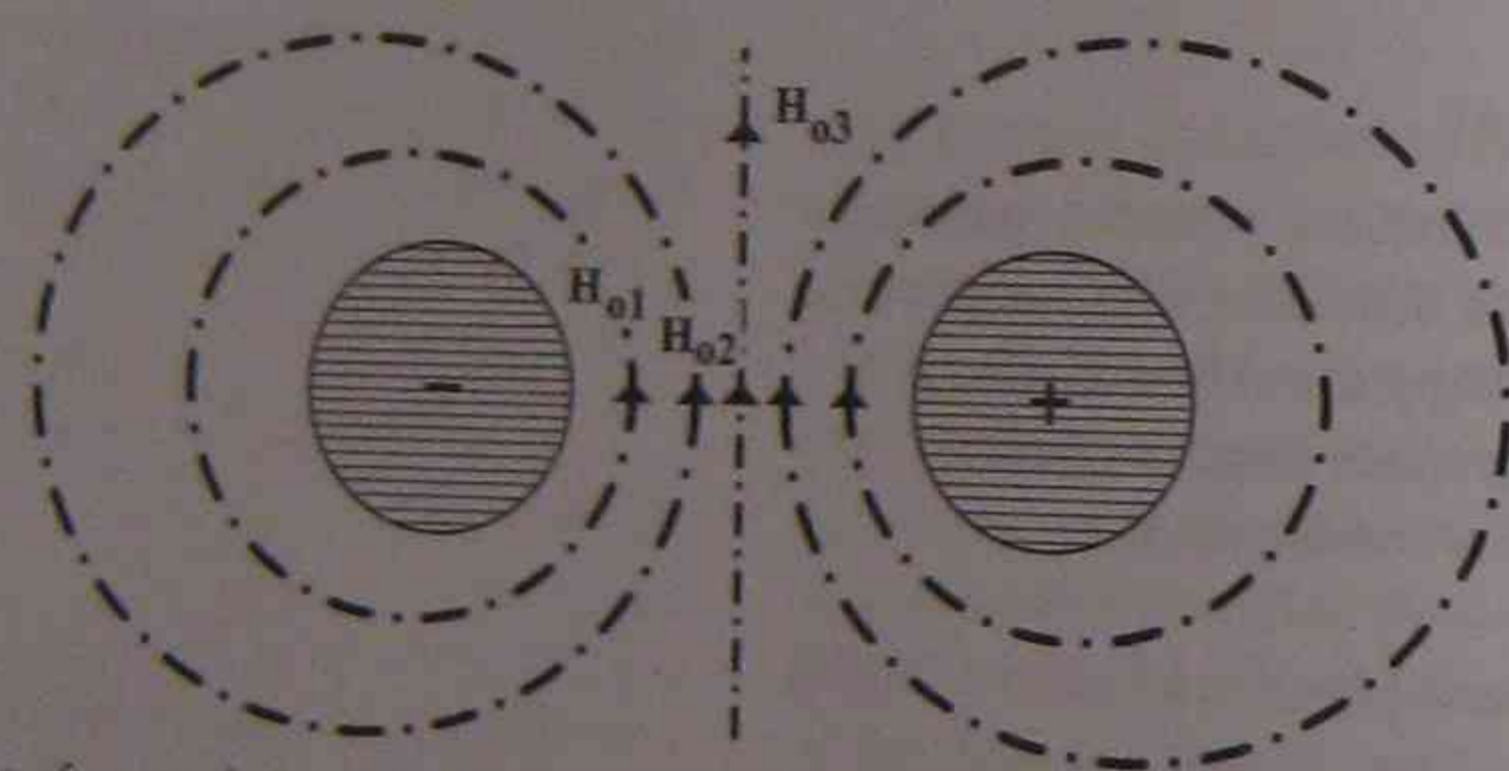**FIGURE 2.4** Magnetic field strength inside and outside of a conductor.

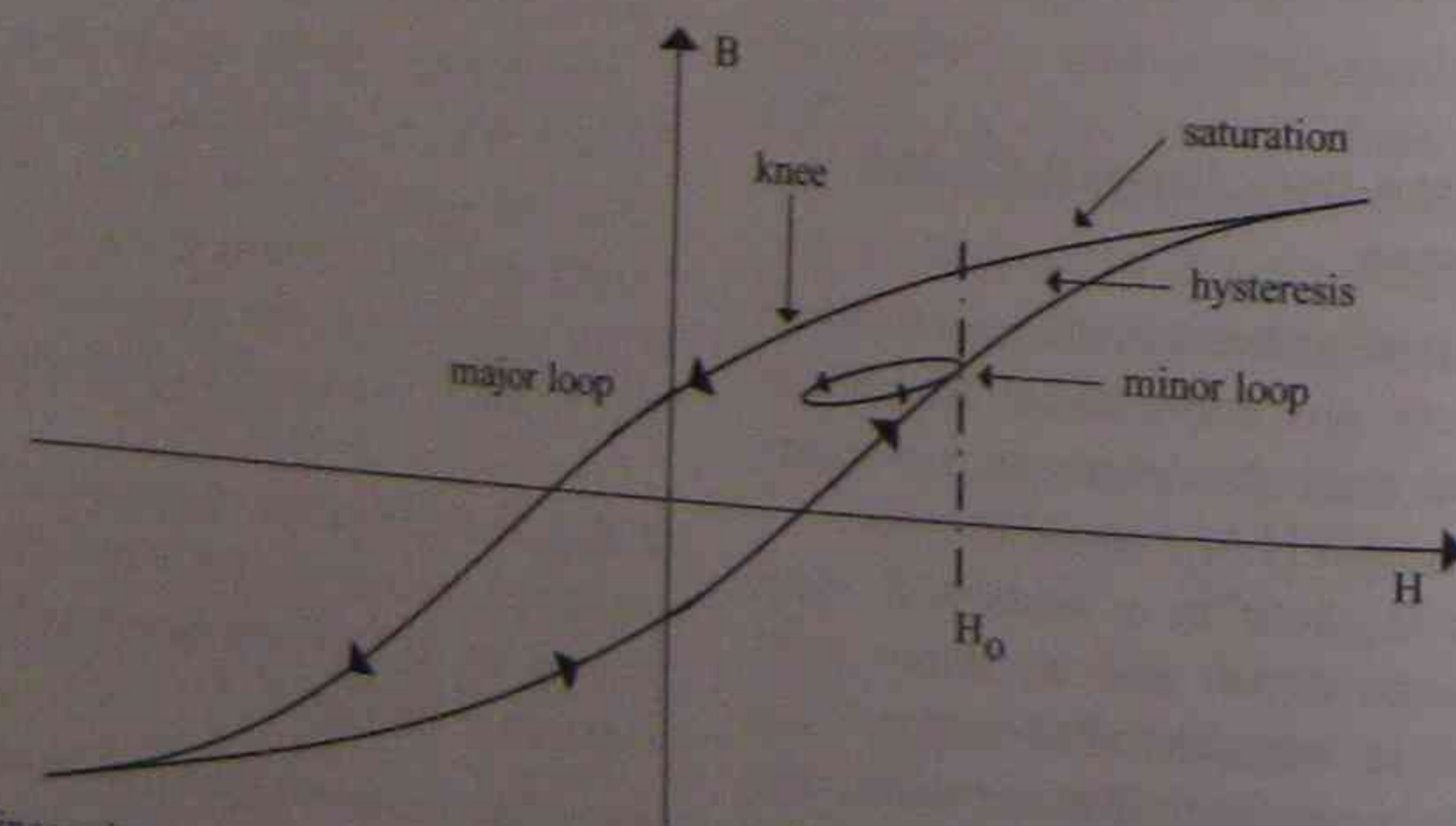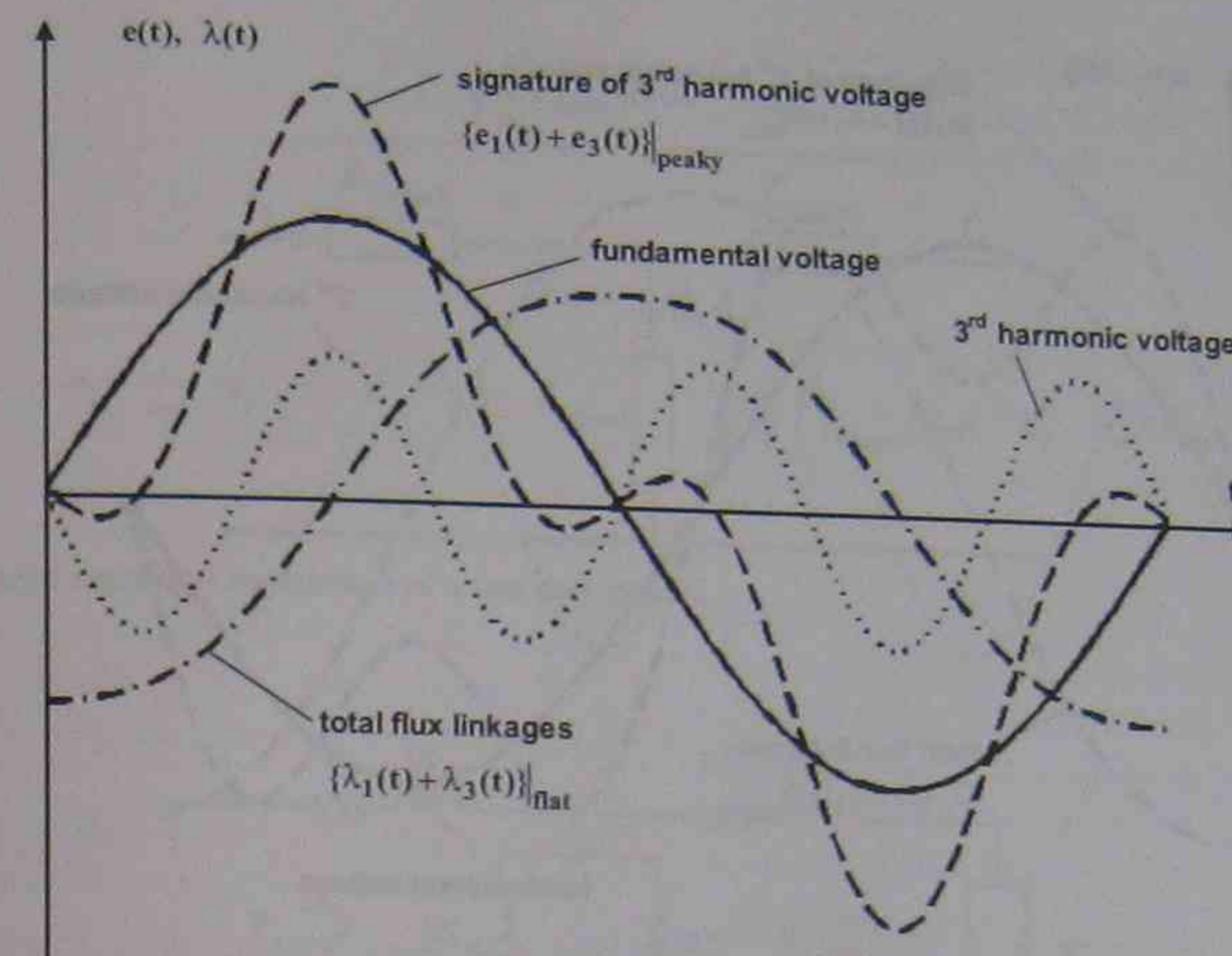**FIGURE 2.5** Distortion of magnetic fields due to proximity effect.

FIGURE 2.6 Nonlinear characteristics of transformer core with major and minor hysteresis loops.

FIGURE E2.1.1 Superposition of fundamental and third harmonic voltages that are in phase (0°, peak-to-peak voltage is maximum).

peak-to-peak value for the total nonsinusoidal voltage. According to Eq. 2-6, the peak-to-peak value of the generated $\lambda(t)$ is minimum, as illustrated by Fig. E2.1.1.

Rule. A "peaky" (peak-to-peak is maximum) voltage $\{e_1(t) + e_3(t)\}$ results in "flat" (peak-to-peak is minimum) flux linkages.

2.2.3.2 Application Example 2.2: Relation between Voltages and Flux Linkages for 180° Phase Shift between Fundamental and Harmonic Voltages

The third harmonic voltage $e_3(t)$ is out of phase (180°) with the fundamental voltage $e_1(t)$. In this case, the total voltage and the resulting flux linkages have minimum and maximum peak-to-peak values, respectively (Fig. E2.2.1).

Rule. A "flat" (peak-to-peak is minimum) voltage $\{e_1(t) + e_3(t)\}$ results in "peaky" (peak-to-peak is maximum) flux linkages.

Generalization. For higher harmonic orders, similar relations between the nonsinusoidal waveforms of induced voltage and flux linkages exist; however, there is an alternating behavior as demonstrated in Table E2.2.1.

This alternating behavior (due to the integral relationship between $e(t)$ and $\lambda(t)$) influences the

TABLE E2.2.1 Phase Relations between Induced Voltages and Flux Linkages when a Harmonic is Superposed with the Fundamental

Harmonic order	Nonsinusoidal voltage $e_1(t) + e_h(t)$	Nonsinusoidal flux linkage $\lambda_1(t) + \lambda_h(t)$
$h = 3$	$\{e_1(t) + e_3(t)\}$ peaky[a]	$\{\lambda_1(t) + \lambda_3(t)\}$ flat[b]
	$\{e_1(t) + e_3(t)\}$ flat	$\{\lambda_1(t) + \lambda_3(t)\}$ peaky
$h = 5$	$\{e_1(t) + e_5(t)\}$ peaky	$\{\lambda_1(t) + \lambda_5(t)\}$ peaky
	$\{e_1(t) + e_5(t)\}$ flat	$\{\lambda_1(t) + \lambda_5(t)\}$ flat
$h = 7$	$\{e_1(t) + e_7(t)\}$ peaky	$\{\lambda_1(t) + \lambda_7(t)\}$ flat
	$\{e_1(t) + e_7(t)\}$ flat	$\{\lambda_1(t) + \lambda_7(t)\}$ peaky
$h = 9$	$\{e_1(t) + e_9(t)\}$ peaky	$\{\lambda_1(t) + \lambda_9(t)\}$ peaky
	$\{e_1(t) + e_9(t)\}$ flat	$\{\lambda_1(t) + \lambda_9(t)\}$ flat
⋮	⋮	⋮

[a] Maximum peak-to-peak value.
[b] Minimum peak-to-peak value.

iron-core (magnetic) losses significantly. Therefore, it is possible that a nonsinusoidal voltage results in less iron-core losses than a sinusoidal wave shape [2]. Note that the iron-core losses are a function of the maximum excursions of the flux linkages (or flux densities B_{max}).

2.2.4 Loss Measurement

For low efficiency ($\eta < 97\%$) devices the conventional indirect loss measurement approach, where the losses P_{loss} are the difference between measured input power P_{in} and measured output power P_{out}, is acceptable. However, for high efficiency ($\eta \geq 97\%$)
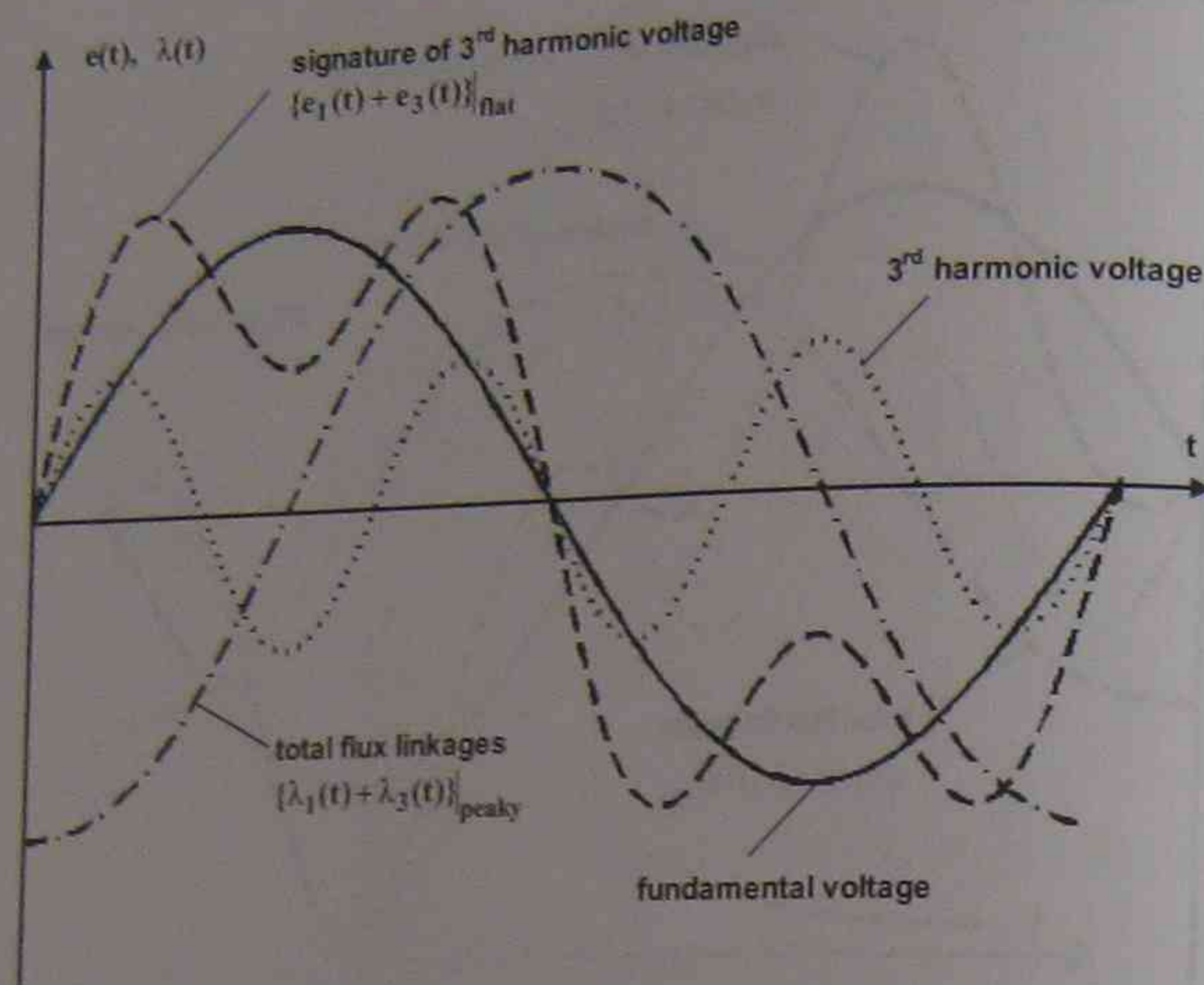
FIGURE E2.2.1 Superposition of fundamental and third harmonic voltages that are out of phase (180°, peak-to-peak voltage is minimum).

devices the indirect loss measurement approach yields losses that have a large error.

2.2.4.1 Indirect Loss Measurement

Consider the two-port system shown in Fig. 2.7:

$$P_{loss} = P_{in} - P_{out}, \qquad (2\text{-}7)$$

or

$$P_{loss} = \frac{1}{T}\int_0^T v_1 i_1 dt - \frac{1}{T}\int_0^T v_2' i_2' dt. \qquad (2\text{-}8)$$

This is the conventional and relatively simple (indirect) technique used for loss measurements of most low-efficiency electric devices under sinusoidal and/or nonsinusoidal operating conditions.

2.2.4.2 Direct Loss Measurement

The two port system of Fig. 2.7 can be specified in terms of series and shunt impedances [1–6], as illustrated in Fig. 2.8.

The powers dissipated in $Z_{series1}$ and $Z'_{series1}$ are

$$P_{series} = \frac{1}{T}\int_0^T P_{series}(t)dt. \qquad (2\text{-}9)$$

The power dissipated in Z_{shunt} is

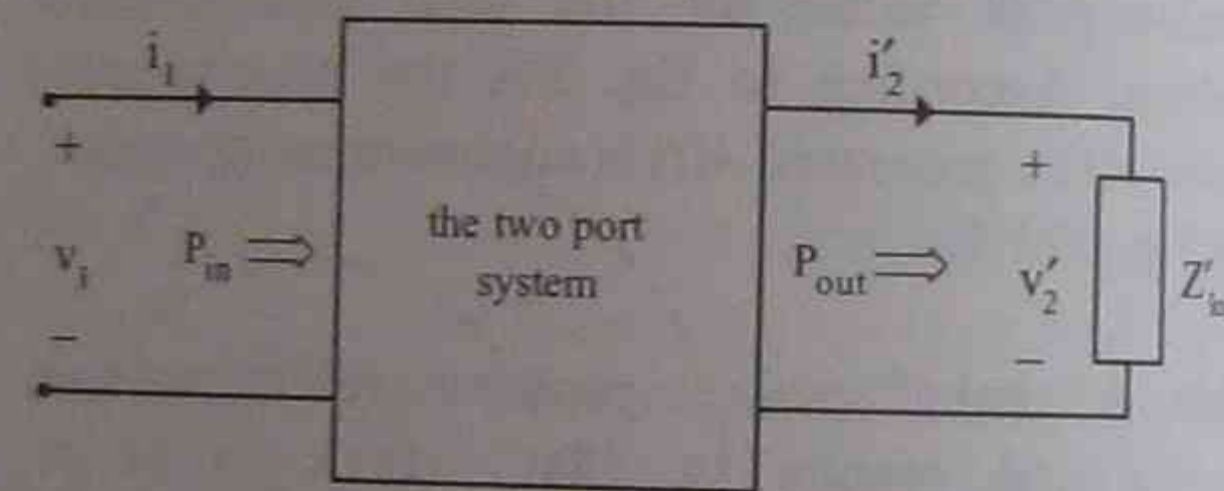$$P_{shunt} = \frac{1}{T}\int_0^T P_{shunt}(t)dt. \qquad (2\text{-}10)$$

FIGURE 2.7 Voltage and current definitions for a two-port system.

Therefore,

$$P_{loss} = P_{series} + P_{shunt} \qquad (2\text{-}11)$$

2.2.4.3 Application Example 2.3: Application of the Direct-Loss Measurement Technique to a Single-Phase Transformer

The direct-loss measurement technique is used to measure losses of a single-phase transformer as illustrated in Fig. E2.3.1 [7].

2.3 DERATING OF SINGLE-PHASE TRANSFORMERS

According to the IEEE dictionary, derating is defined as "the intentional reduction of stress/strength ratio (e.g., real or apparent power) in the application of an item (e.g., transformer), usually for the purpose of reducing the occurrence of stress-related failure (e.g., reduction of lifetime of transformer due to
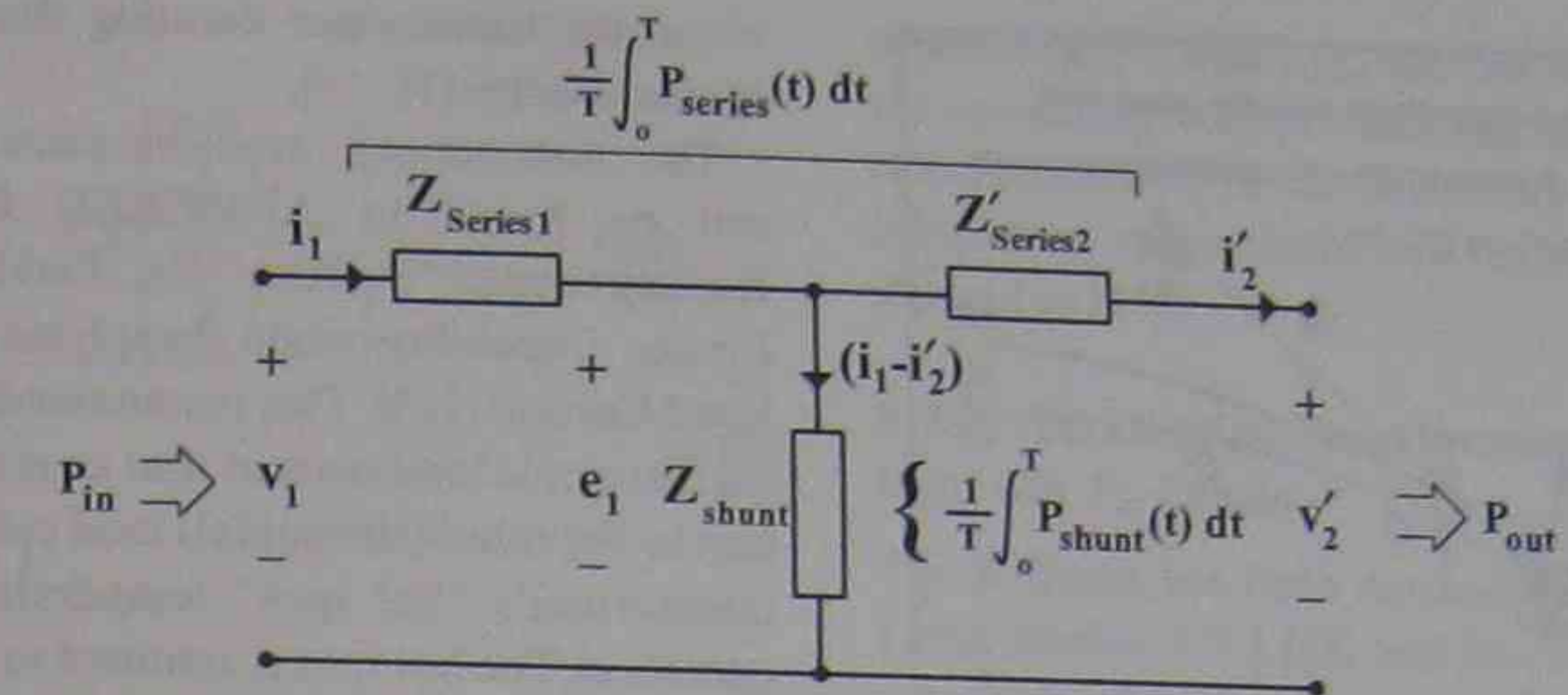
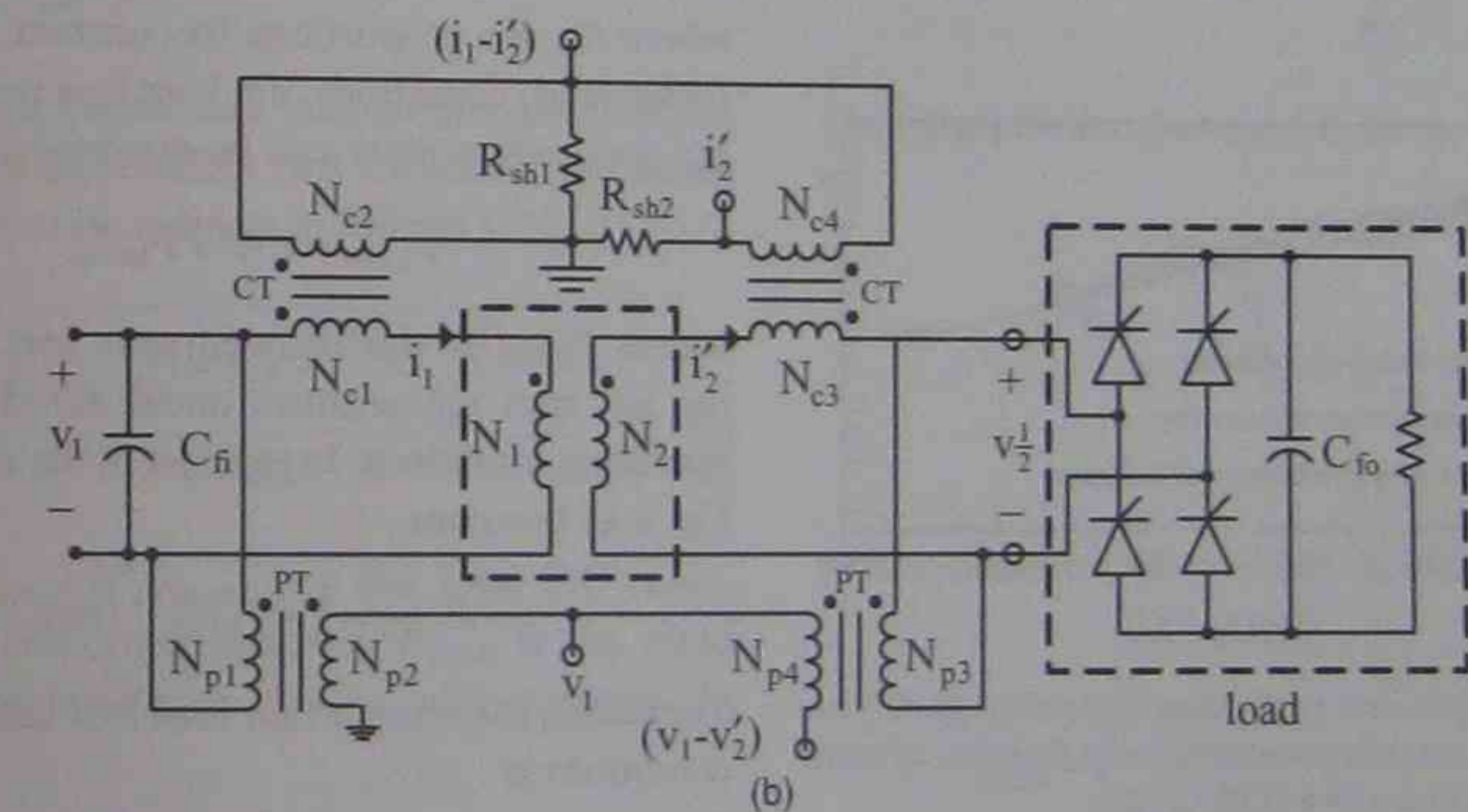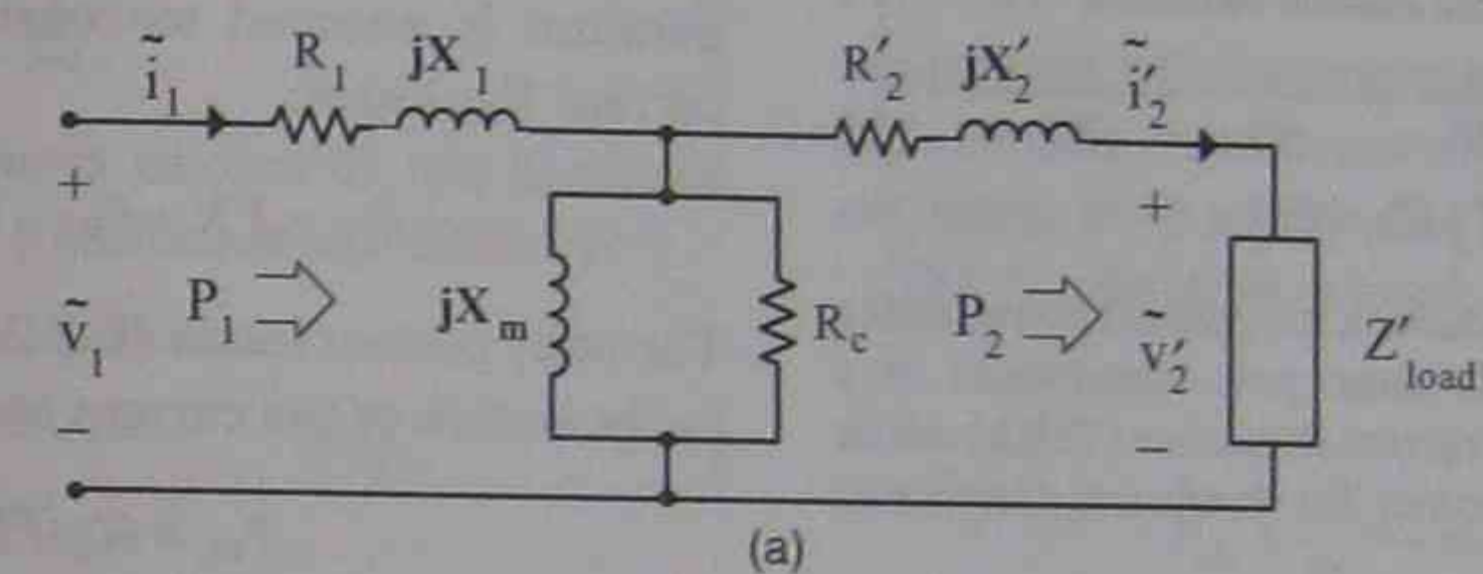FIGURE 2.8 Series and shunt impedances of a two-port system.

FIGURE E2.3.1 Application of direct-loss measurement technique to a single-phase transformer; (a) equivalent circuit, (b) measuring circuit.

increased temperature beyond rated temperature)." As has been discussed in Section 2.2 harmonic currents and voltages result in harmonic losses increasing the temperature rise. This rise beyond its rated value results in a reduction of lifetime [10] as will be discussed in Chapter 6. For transformers two derating parameters can be defined:

- reduction in apparent power rating (RAPR), and
- real power capability (RPC).

Although the first one is independent of the power factor, the second one is strongly influenced by it.

2.3.1 Derating of Transformers Determined from Direct-Loss Measurements

The direct-loss measurement technique of Section 2.2.4.2 is applied and the reduction of apparent power (RAPR) is determined such that for any given total harmonic distortion of the current (THD$_i$), the rated losses of the transformer will not be exceeded.
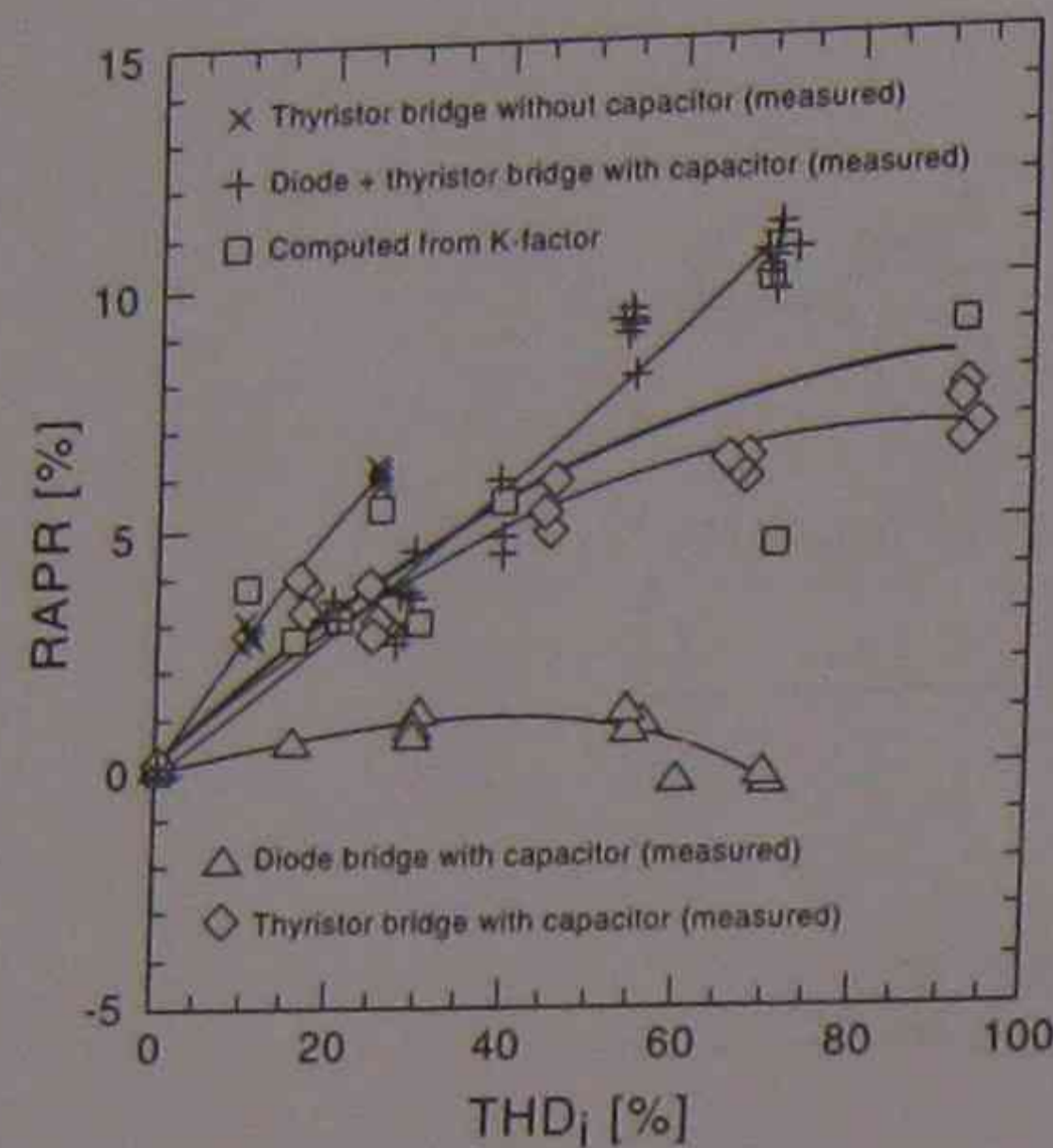
FIGURE 2.9 Measured reduction in apparent power rating (RAPR) of 25 kVA single-phase pole transformer as a function of total harmonic current distortion (THD_i) where 3rd and 5th current harmonics are dominant. Calculated values from K-factor [12].
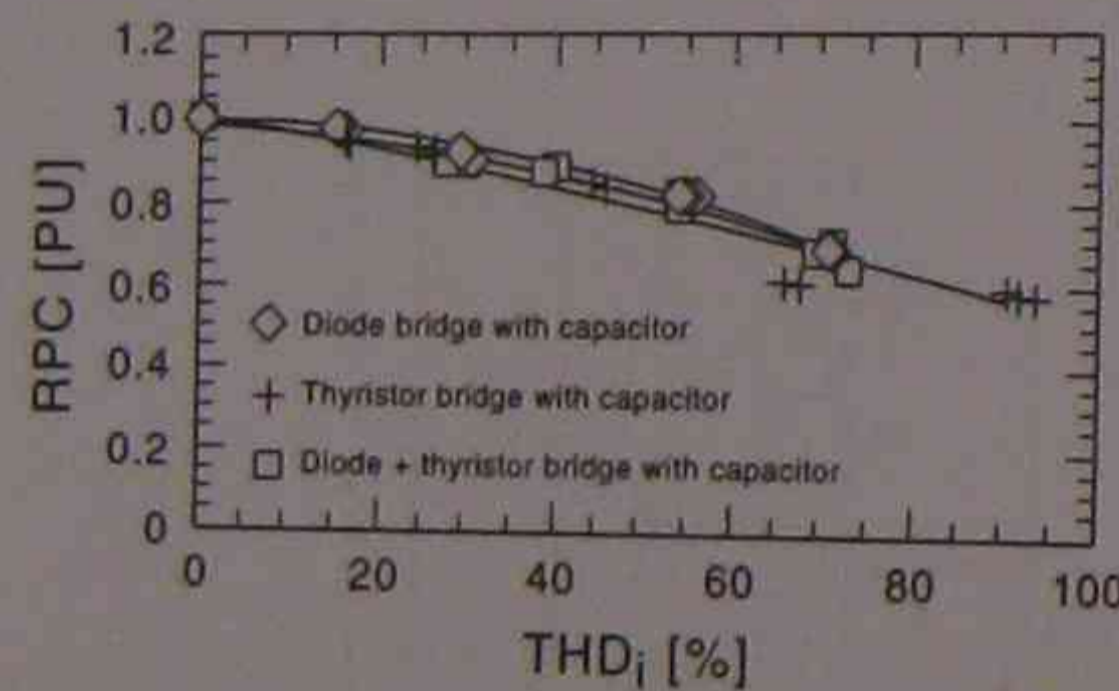

FIGURE 2.10 Measured real power capability (RPC) of 25 kVA single-phase pole transformer as a function of total harmonic current distortion (THD_i) [12].

Figures 2.9 and 2.10 show the RAPR and RPC as a function of the THD_i.

2.3.2 Derating of Transformers Determined from the K-Factor

It is well known that power system transformers must be derated when supplying nonlinear loads. Transformer manufacturers have responded to this problem by developing transformers rated for 50% or 100% nonlinear load. However, the impact of nonlinear loads on transformers greatly depends on the nature and the harmonic spectrum caused by the nonlinear load, which is not considered by the manufacturers. The K-factor rating is an alternative tech-

nique for transformer derating that includes load characteristics [11, 13].

The assumptions used in calculating K-factor can be found in ANSI/IEEE C57.110, IEEE Recommended Practice for Establishing Transformer Capability when Supplying Nonsinusoidal Load Currents [13]. This recommendation calculates the harmonic load current that causes losses equivalent to the rated (sinusoidal) load current so that the transformer's "hot spot" temperature will not be exceeded. The hot spot is assumed to be where eddy-current losses are the greatest and the coolant (oil) is hottest (e.g., at the inner low-voltage winding).

The load loss (LL) generating the hot spot temperature is assumed to consist of I^2R and eddy-current P_{EC} losses:

$$P_{LL} = I^2R + P_{EC} \quad \text{(watts)}. \quad (2\text{-}12)$$

The eddy current losses (Eq. 2–12) are proportional to the square of the current and frequency:

$$P_{EC} = K_{EC}I^2h^2, \quad (2\text{-}13)$$

where K_{EC} is a proportionality constant. Under rated (sinusoidal) conditions, the load loss resulting in the hot spot temperature can be expressed as

$$P_{LL\text{-}R} = I^2R^2 + P_{EC\text{-}R}, \quad (2\text{-}14)$$

where $P_{EC\text{-}R}$ is the eddy-current loss resulting in the hot spot temperature under rated (sinusoidal) operating conditions. In per unit of the rated I^2R loss, Eq. 2-14 becomes

$$P_{LL\text{-}R} = 1 + P_{EC\text{-}R} \quad \text{(pu)}. \quad (2\text{-}15)$$

Therefore, the transformer load loss under harmonic conditions is

$$P_{LL} = \sum_{h=1}^{h\max} I_h^2 + \left(\sum_{k=1}^{h\max} I_h^2 h^2\right) P_{EC\text{-}R} \quad \text{(pu)}. \quad (2\text{-}16)$$

The first and second terms on the right side of the above equation represent the I^2R loss and the eddy-current loss, respectively. Setting $P_{LL} = P_{LL\text{-}R}$ gives

$$1 + P_{EC\text{-}R} = \sum_{h=1}^{h\max} I_h^2 + \left(\sum_{h=1}^{h\max} I_h^2 h^2\right) P_{EC\text{-}R} \quad \text{(pu)}. \quad (2\text{-}17)$$

Now, if we define the K-factor as follows [13]:

$$K = \frac{\sum_{h=1}^{h\max} I_h^2 h^2}{I_R^2} \quad \text{(pu)}, \quad (2\text{-}18)$$

then

$$1 + P_{EC\text{-}R} = \sum_{h=1}^{h\max} I_h^2 + K\left(\frac{\sum_{h=1}^{h\max} I_h^2}{\sum_{h=1}^{h\max} I_h^2}\right) I_R^2 P_{EC\text{-}R} \quad \text{(pu)}. \quad (2\text{-}19)$$

Solving for $\sum_{h=1}^{h\max} I_h^2$,

$$\sum_{h=1}^{h\max} I_h^2 = \frac{1 + P_{EC\text{-}R}}{1 + K\frac{I_R^2}{\sum_{h=1}^{h\max} I_h^2}(P_{EC\text{-}R})} \quad \text{(pu)}. \quad (2\text{-}20)$$

Therefore, the maximum amount of rms harmonic load current that the transformer can deliver is

$$I_{\max}^{pu} = \sqrt{\frac{1 + P_{EC\text{-}R}}{1 + K\frac{I_R^2}{\sum_{h=1}^{h\max} I_h^2}[(P_{EC\text{-}R})]}} \quad \text{(pu)}. \quad (2\text{-}21)$$

Using the K-factor and transformer parameters, the maximum permissible rms current of the transformer can also be defined as follows [11]:

$$I_{\max}^{p.u.} = \sqrt{\frac{R_{DC} + R_{EC\text{-}R}(1-K) - \frac{(\Delta P_{fe} + \Delta P_{OSL})}{I_R^2}}{R_{DC}}}. \quad (2\text{-}22)$$

$R_{DC} = R_{DCprimary} + R'_{DCsecondary}$ is the total DC resistance of a transformer winding. $R_{EC\text{-}R}$ is the rated pu additional resistance due to eddy currents. In addition,

$$\Delta P_{fe} = \sum_{h=1}^{h\max} P_{feh} - P_{feR},$$

and

$$\Delta P_{OSL} = \sum_{h=1}^{h\max} P_{OSLh} - P_{OSLR}.$$

ΔP_{fe} is the difference between the total iron core losses (including harmonics) and the rated iron core losses without harmonics. ΔP_{OSL} is the difference between the total other stray losses (OSL) including harmonics and the rated other stray losses without harmonics.

The reduction of apparent power (RAPR) is

$$RAPR = 1 - (V_{2rms}^{nonlinear}/V_{2rms}^{rat}) I_{\max}^{p.u.}, \quad (2\text{-}23)$$

where $V_{2rms}^{nonlinear}$ and V_{2rms}^{rat} are the total rms value of the secondary voltage including harmonics and the rated rms value of the secondary winding without harmonics, respectively. All above parameters are defined in [11].

2.3.3 Derating of Transformers Determined from the F_{HL}-Factor

The K-factor has been devised by the Underwriters Laboratories (UL) [13] and has been recognized as a measure for the design of transformers feeding nonlinear loads demanding nonsinusoidal currents. UL designed transformers are K-factor rated. In February 1998 the IEEE C57.110/D7 [14] standard was created, which represents an alternative approach for assessing transformer capability feeding nonlinear loads. Both approaches are comparable [15].

The F_{HL}-factor is defined as

$$F_{HL} = \frac{P_{EC}}{P_{EC\text{-}O}} = \frac{\sum_{h=1}^{h\max} I_h^2 h^2}{\sum_{h=1}^{h\max} I_h^2}. \quad (2\text{-}24)$$

Thus the relation between K-factor and F_{HL}-factor is

$$K = \left(\frac{\sum_{h=1}^{h\max} I_h^2}{I_R^2}\right) F_{HL}, \quad (2\text{-}25)$$

or the maximum permissible current is [15]

$$I_{\max}^{p.u.} = \sqrt{\frac{R_{DC} + R_{EC\text{-}R} - \frac{\Delta P_{Fe} + \Delta P_{osl}}{I_R^2}}{R_{DC} + F_{HL}R_{EC\text{-}R}}}, \quad (2\text{-}26)$$

and the reduction in apparent power rating (RAPR) is

$$RAPR = 1 - \left(\frac{V_{2rms}^{nonlinear}}{V_{2rms}^{rat}}\right) I_{\max}^{p.u.}. \quad (2\text{-}27)$$

The RAPR as a function of F_{HL} is shown in Fig. 2.11.

2.3.3.1 Application Example 2.4: Sensitivity of K- and F_{HL}-Factors and Derating of 25 kVA Single-Phase Pole Transformer with Respect to the Number and Order of Harmonics

The objective of this example is to show that the K- and F_{HL}-factors are a function of the number and order of harmonics considered in their calculation.

61) Masoum, M.A.S.; Ladjevardi, M.; Jafarian, A.; and Fuchs, E.F.; "Optimal placement, replacement and sizing of capacitor banks in distorted distribution networks by genetic algorithms," *IEEE Transactions on Power Delivery*, Vol. 19, No. 4, October 2004, pp. 1794–1801.

62) Fuchs, E.F.; "Are harmonic recommendations according to IEEE 519 and CEI/IEC too restrictive?" *Proceedings of Annual Frontiers of Power Conference*, Oklahoma State University, Stillwater, Oklahoma, Oct. 28–29, 2002, pp. IV-1 to IV-18.

63) Standard ANSI/IEEE Std C57.110.

64) Duffey, C.K.; and Stratford, R.P.; "Update of harmonic standard IEEE-519: IEEE recommended practices and requirements for harmonic control in power systems", *IEEE Transactions on Industry Applications*, Vol. 25, No. 6, Nov./Dec. 1989, pp. 1025–1034.

65) www.ballard.com.

66) "The road ahead for EV batteries," *ERPI Journal*, March/April 1996.

67) Wang, C.; Nehrir, M.H.; and Shaw, S.R.; "Dynamic models and model validation for PEM fuel cells using electrical circuits," *IEEE Transactions on Energy Conversion*, Vol. 20, No. 2, June 2005, pp. 442–451.

1.12 ADDITIONAL BIBLIOGRAPHY

68) Fuchs, E.F.; You, Y.; and Roesler, D.J.; "Modeling, simulation and their validation of three-phase transformers with three legs under DC bias," *IEEE Transactions on Power Delivery*, Vol. 14, No. 2, April 1999, pp. 443–449.

69) Fardoun, A.A.; Fuchs, E.F.; and Huang, H.; "Modeling and simulation of an electronically commutated permanent-magnet machine drive

system using SPICE," *IEEE Transactions on Industry Applications*, July/August 1994, Vol. 30, No. 4, July/August 1994, pp. 927–937.

70) Fuchs, E.F.; Lin, D.; and Martynaitis, J.; "Measurement of three-phase transformer derating and reactive power demand under nonlinear loading conditions," *IEEE Transactions on Power Delivery*, Vol. 21, Issue 2, April 2006, pp. 665–672.

71) Fuchs, E.F.; Roesler, D.J.; and Kovacs, K.P.; "Aging of electrical appliances due to harmonics of the power system's voltage," *IEEE Transactions on Power Delivery*, July 1986, Vol. TPWRD-1, No. 3, pp. 301–307.

72) Fuchs, E.F.; and Hanna, W.J.; "Measured efficiency improvements of induction motors with thyristor/triac controllers," *IEEE Transactions on Energy Conversion*, Vol. 17, No. 4, December 2002, pp. 437–444.

73) Lin, D.; and Fuchs, E.F.; "Real-time monitoring of iron-core and copper losses of three-phase transformer under (non)sinusoidal operation," *IEEE Transactions on Power Delivery*, Vol. 21, No. 3, July 2006, pp. 1333–1341.

74) Yildirim, D.; and Fuchs, E.F.; "Commentary to various formulations of distortion power D," *IEEE Power Engineering Review*, Vol. 19, No. 5, May 1999, pp. 50–52.

75) Fuchs, E.F.; and Fei, R.; "A New computer-aided method for the efficiency measurement of low-loss transformers and inductors under nonsinusoidal operation," *IEEE Transactions on Power Delivery*, January 1996, Vol. PWRD-11, No. 1, pp. 292–304.

76) Fuchs, E.F.; Roesler, D.J.; and Masoum, M.A.S.; "Are harmonic recommendations according to IEEE and IEC too restrictive?" *IEEE Transactions on Power Delivery*, Vol. 19, No. 4, Oct. 2004, pp. 1775–1786.

Harmonic Models of Transformers

Extensive application of power electronics and other nonlinear components and loads creates single-time (e.g., spikes) and periodic (e.g., harmonics) events that could lead to serious problems within power system networks and its components (e.g., transformers). Some possible impacts of poor power quality on power transformers are

- saturating transformer core by changing its operating point on the nonlinear $\lambda - i$ curve,
- increasing core (hysteresis and eddy current) losses and possible transformer failure due to unexpected high losses associated with hot spots,
- increasing (fundamental and harmonic) copper losses,
- creating half-cycle saturation in the event of even harmonics and DC current,
- malfunctioning of transformer protective relays,
- aging and reduction of lifetime,
- reduction of efficiency,
- derating of transformers,
- decrease of the power factor,
- generation of parallel (harmonic) resonances and ferroresonance conditions, and
- deterioration of transformers' insulation near the terminals due to high voltage stress caused by lightning and pulse-width-modulated (PWM) converters.

These detrimental effects call for the understanding of how harmonics affect transformers and how to protect them against poor power quality conditions. For a transformer, the design of a harmonic model is essential for loss calculations, derating, and harmonic power flow analysis.

This chapter investigates the behavior of transformers under harmonic voltage and current conditions, and introduces harmonic transformer models suitable for loss calculations, harmonic power flow analysis, and computation of derating functions. After a brief introduction of the conventional (sinusoidal) transformer model, transformer losses with emphasis on the impacts of voltage and current harmonics are presented. Several techniques for the computation of single-phase transformer derating

factors (functions) are introduced. Thereafter, a survey of transformer harmonic models is given. In subsequent sections, the issues of ferroresonance, geomagnetically induced currents (GICs), and transformer grounding are presented. A section is also provided for derating of three-phase transformers.

2.1 SINUSOIDAL (LINEAR) MODELING OF TRANSFORMERS

Transformer simulation under sinusoidal operating conditions is a well-researched subject and many steady-state and transient models are available. However, transformer cores are made of ferromagnetic materials with nonlinear B–H ($\lambda - i$) characteristics. They exhibit three types of nonlinearities that complicate their analysis: saturation effect, hysteresis (major and minor) loops, and eddy currents. These phenomena result in nonsinusoidal flux, voltage and current waveforms on primary and secondary sides, and additional copper (due to current harmonics) and core (due to hysteresis loops and eddy currents) losses at fundamental and harmonic frequencies. Linear techniques for transformer modeling neglect these nonlinearities (by assuming a linear $\lambda - i$ characteristic) and use constant values for the magnetizing inductance and the core-loss resistance. Some more complicated models assume nonlinear dependencies of hysteresis and eddy-current losses with fundamental voltage magnitude and frequency, and use a more accurate equivalent value for the core-loss resistance. Generally, transformer total core losses can be approximated as

$$P_{fe} = P_{hys} + P_{eddy} = K_{hys}(B_{max})^s f + K_{eddy}(B_{max})^2 f^2, \quad (2\text{-}1)$$

where P_{hys}, P_{eddy}, B_{max}, and f are hysteresis losses, eddy-current losses, maximum value of flux density, and fundamental frequency, respectively. K_{hys} is a constant for the grade of iron employed and K_{eddy} is the eddy-current constant for the conductive material. S is the Steinmetz exponent ranging from 1.5 to 2.5 depending on the operating point of transformer core.